University of Baghdad
College of Engineering
JOURNAL OF ENGINEERING

Journal of Engineering

journal homepage: www.joe.uobaghdad.edu.iq

Volume 29 Number 8 August 2023

Impact of Anchored CFRP Composites on the Strengthening of Partially Damaged PC Girders

Hayder Qays Abbas[1,*], Alaa Hussein Al-Zuhairi[2]

Department of Civil Engineering, College of Engineering, University of Baghdad, Baghdad, Iraq
haider_q@yahoo.com[1], alaalwn@coeng.uobaghdad.edu.iq[2]

ABSTRACT

This manuscript investigated the effect of anchorage CFRP wrapping sheets, bolts, and laminate interlock on increasing the efficiency of flexural strengthening for the post-tension girder using CFRP composites techniques longitudinal laminates at the soffit for partially damaged loss of about 14.3% from its area of prestressed concrete beams, and the impact on restoring the original flexural capacity of PC girder. Mitigating delamination of the soffit of horizontal laminates (CFRP). The texture of the laminate and anchorages influenced the stress of the laminate carbon fiber, the mode of crack propagation and failure, and consequently, the beam's attitude has been investigated in this manuscript. The experimental findings demonstrated that using CFRP laminates significantly affects strand strain, especially when anchorage wrapping is applied. The laminates CFRP-EB enhanced the flexural capacity by around 13% of the original strength, which equates to a 13% increase in strand damage. Despite an increase in flexural capacity of 20%, 22%, and 29% when using anchorage wrapping, mechanical bolts, and laminate interlock, respectively. It has been proposed to use quasi-experimental equations to predicate the actual stress of un-grouted strands, considering the influence of CFRP laminate and wrapping anchorage sheets techniques only. The experiment outcomes demonstrated that using Anchored CFRP significantly affects load-carrying capacity and cracking load by up to 29% and delays the bonding failure.

Keywords: CFRP Laminate, CFRP sheet, Debonding, Post Tensioned Girder, Strand Damage.

*Corresponding author
Peer review under the responsibility of University of Baghdad.
https://doi.org/10.31026/j.eng.2023.08.08

Article received: 07/10/2022
Article accepted: 24/10/2022
Article published: 01/08/2023

تأثير استعمال مثبتات الياف الكاربون البوليمرية في تقوية العتبات الخرسانية سابقة الاجهاد المعرضة الى التلف الجزئي

حيدر قيس عباس[1]،*، علاء حسين الزهيري[2]

قسم الهندسة المدنية، كلية الهندسة، جامعة بغداد، بغداد، العراق

الخلاصة

تتناول هذه الدراسة تأثير استخدام مثبتات التقوية (الرواسي) مثل اللف النسيجي والمسامير الميكانيكية واستخدام التعشيق لصفائح الكاربون المثبتة أسفل العتبات على زيادة كفاءة استخدام مركبات الكاربون البوليمرية في تقوية الانحناء والمثبتة بشكل طولي أسفل العتبات والتي تكون معرضة الى تلف جزئي في الجدائل حوالي 14.3٪ من مساحة ضفائر الشد الفولاذية، وتأثير التقوية (التدعيم) على استعادة القدرة التصميمة للعتبات سابقة الاجهاد. وتتضمن دراسة المتغيرات الخاصة بالصفائح الأفقية CFRP وتأثيرها على المقاومة للمقاطع. بالإضافة الى تأثير استخدام المثبتات (الرواسي) على الاجهادات المسلطة على المقاطع، وكذلك تطور التشققات وانماط الفشل. أظهرت النتائج التجريبية أن استخدام رقائق البوليمر المقوى بألياف الكربون له تأثير كبير على انفعال ضفائر الشد، حيث أظهرت النتائج التجريبية أن استخدام رقائق البوليمر المقوى بألياف الكربون له تأثير كبير على إجهاد الضفائر، خاصة عند تطبيق اللف النسيجي. عززت صفائح الكاربون فايبر البوليمرية والملصقة خارجيا قدرة الانحناء بحوالي 13٪، لنسبة ضفائر تالفة بحوالي 13٪ من المساحة الكلية للضفائر. بالإضافة الى ذلك فقد اظهرت الدراسة زيادة قدرة الانحناء بنسبة 20٪، 22%, 29٪ عند استخدام اللف النسيجي، والمسامير الميكانيكية، والتعشيق لصفائح الكاربون على التوالي. تم اقتراح استخدام معادلات شبه تجريبية لتقدير الضغط الفعلي للضفائر الغير محشو، مع الأخذ في الاعتبار تأثير استخدام صفائح الكاربون واستخدام تقنية اللف النسيجي. وقد أظهرت النتائج التجريبية أن استخدام الرواسي له تأثير واضح وكبير على زيادة في قابلية تحمل الاحمال كذلك حمل التشقق وبنسبة تصل الى 29% بالإضافة الى تأخير عملية الفصل.

الكلمات الرئيسية: عتبات مسبقة الاجهاد، الفصل، تلف القابلات، صفائح الكاربون فايبر، انسجة الكاربون فايبر.

1. INTRODUCTION

High-speed car collisions have impacted several bridges, which can cause the concrete and/or strands to fail. Globally, pre-stressed (PS) concrete structural components are corroding and creating discomfort (**Abdulkareem and Izzat, 2022)**. Neoteric destructive failures have necessitated a reevaluation of the condition of several pre-stressed members **(Al-Hilali et al., 2022)**. Spawned new postings and, in certain instances, emergency closures. Some collapse and destruction result from explosive-based terrorist assaults **(Abdulkareem et al., 2021)**, which damage pre-stressed bridge structural components or tendons (**Hekmet and Izzet, 2019)**. The loss of strands on the concrete member significantly impacts the design prestressed force, indicating a decrease in nominal capacity and lack of serviceability **(Razaqpur and Mostafa, 2015).** In this publication, one of the strengthening discoveries that will be studied is the usage of CFRP-laminate with and without anchorage to improve the laminate used for strengthening. Carbon fiber reinforced

polymers (CFRP) are increasingly utilized to reinforce and repair reinforced concrete (RC) constructions. The advantages of employing FRP include the application's ease of use, the material's high ultimate strength **(Daraj and Al-Zuhairi, 2022)**, and its corrosion resistance; corrosion is the leading source of bridge damage. Experiment results indicate that the maximal strength of prestressed externally reinforced beams with CFRP laminate is not always fully reached due to premature degradation of laminate carbon fiber from the concrete substrate. In the last several decades, external fiber-reinforced polymer (FRP) composites have evolved as a feasible alternative to one of the standard strengthening methods **(Qays and Al-Zuhairi, 2022)**. Pre-tensioning girder structures with FRP composites has occurred. Guidelines for using the FRP technique in the reinforcing steel of post-tensioned PC structural systems have been thoroughly tested during the previous two years **(Oukaili and Buniya, 2013)**. Sadly, this is because it is difficult to determine stress and strain in unbonded tendons at peak of flexural capacity due to the lack of tendons contact relative to the surrounding concrete **(Nguyen-Minh et al., 2018)**. In reality, it is better to eliminate or transform the brittle failure mode into a ductile failure mode. Using metallic or CFRP anchors to secure the laminate to the concrete substrate may be a realistic method for doing this **(Razaqpur and Mostafa, 2015)**. The CFRP U-wrapped anchors or any other mechanical anchor systems were utilized and showed excellent effectiveness in delaying the delamination process and boosting the efficiency of the strengthening **(Abbas and Al-Zuhairi, 2022)**.

The overarching goal of this study was to establish recommendations on how to restore the flexural capacity of prestressed girders exposed to partially damaged strands using anchored CFRP strengthening techniques as well as the effectiveness of bonding enhancement techniques in using anchorage sheets, bolts, and other types of anchorage.

2. SPECIMEN DETAIL AND SETUP

This study employs seven girders, as depicted in **Table 1**. The overall length is 3000 mm, and support by simple ends (hinge and roller) is 2800 mm distant with 2-ϕ16mm rebars at the bottom, while for the compression zone 2-ϕ10 mm are equipped (non-continuous), stirrups reinforcement was designed by using 10mm rebars with spacing as indicated in **Figure 1**. PVC conduit is employed to occupy the strand with a diameter equal to 22.5 mm consisting of end grips utilizing two unbonded strands that stretch 500mm from each side. All tests were conducted in the laboratory of Baghdad University's College of Engineering under four points of loading, as depicted in **Figs. 1 to 3**. CFRP Laminates (50mm and 1.2mm for the width and thickness respectively) are affixed to the soffit to reinforce the specimen.

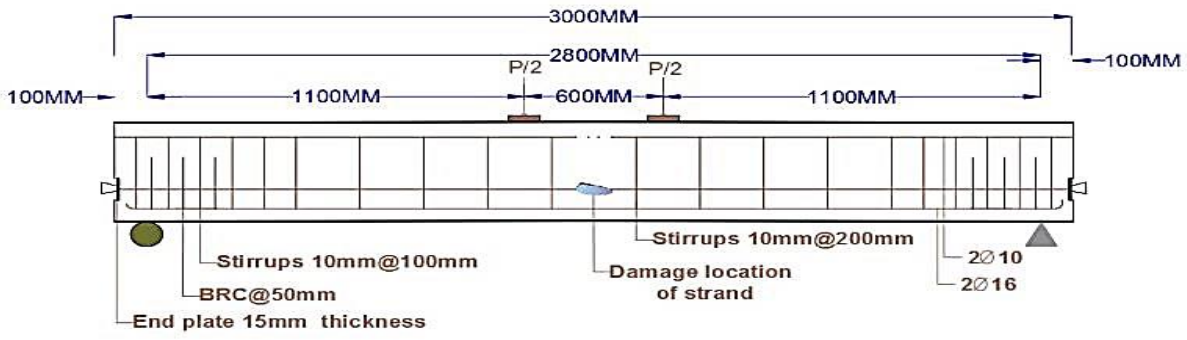

Figure 1. Member detail and damage location of strands

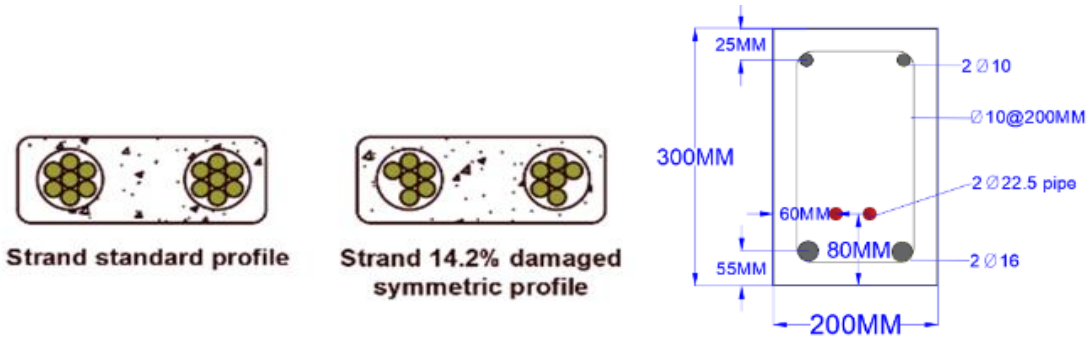

a-undamaged strand layout **b-**damaged strand layout **c-** cross section

Figure 2. Cross-sectional detail and strand damage **a-**undamaged strand layout, **b-**damaged strand layout, **c-** cross-section

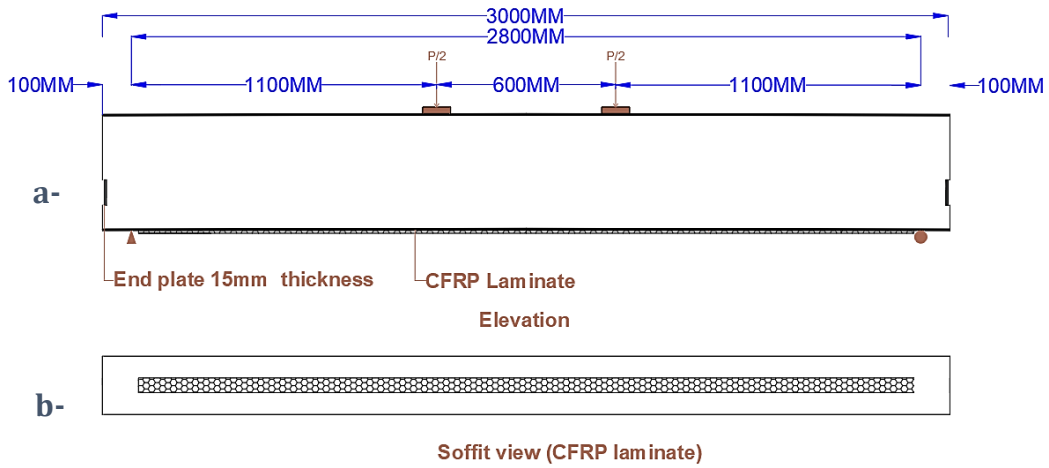

Figure 3. Laminate location, a- elevation b- soffit view

The anchorage sheet thickness is 0.167mm built up on a U-wrapping form while the anchorage interlock laminate that is coupled is divided into three strips attached in the transverse direction at the soffit, 16mm of bolts diameter have been used for the mechanical anchorage techniques as illustrated in **Fig. 4 to 7**.

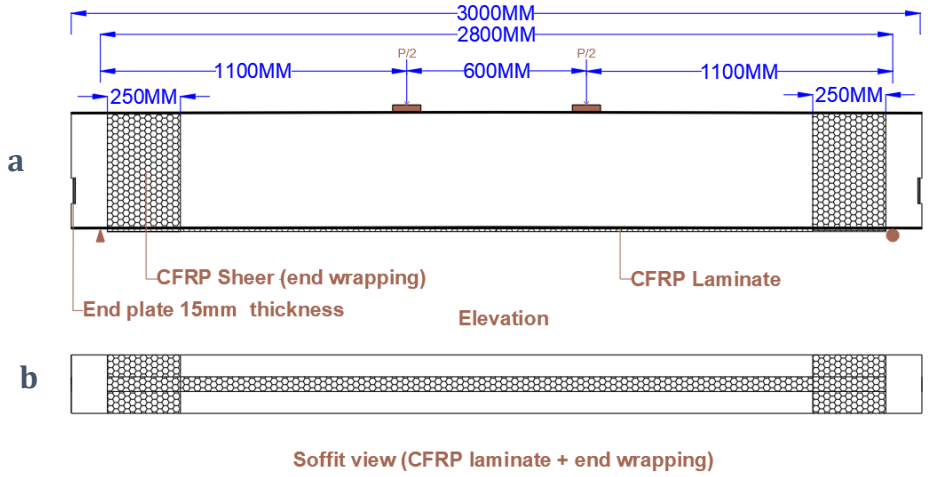

Figure 4. Laminate and end sheet anchorage, a- elevation b- soffit view

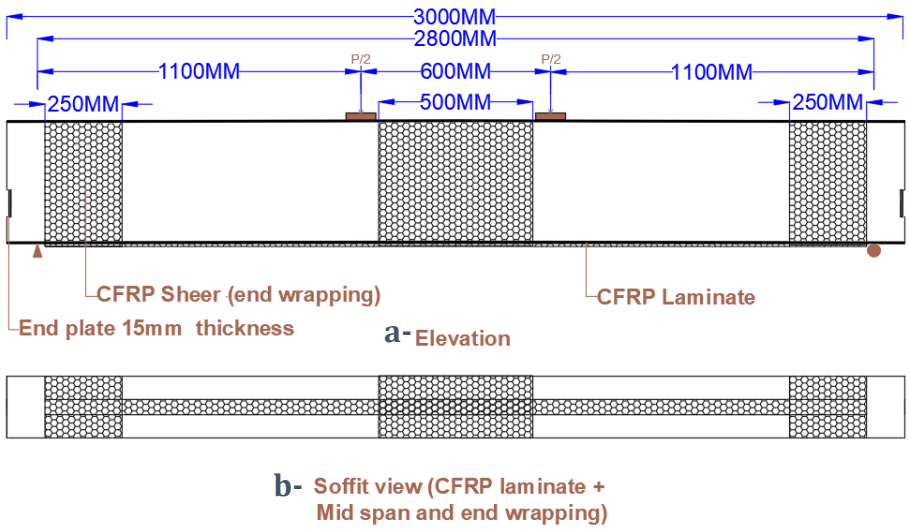

Figure 5. Laminate with middle and end sheet anchorage, a- elevation b- soffit view

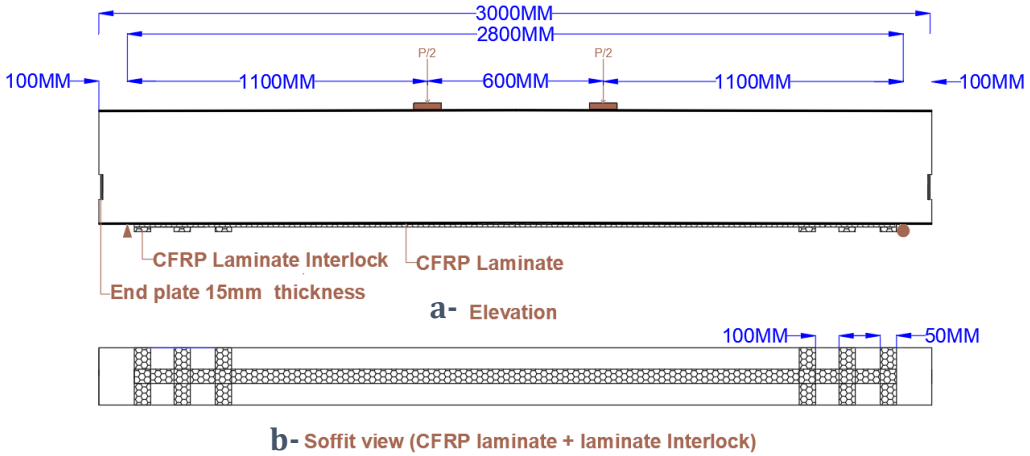

Figure 6. Laminate with interlock anchorage, a- elevation b- soffit view

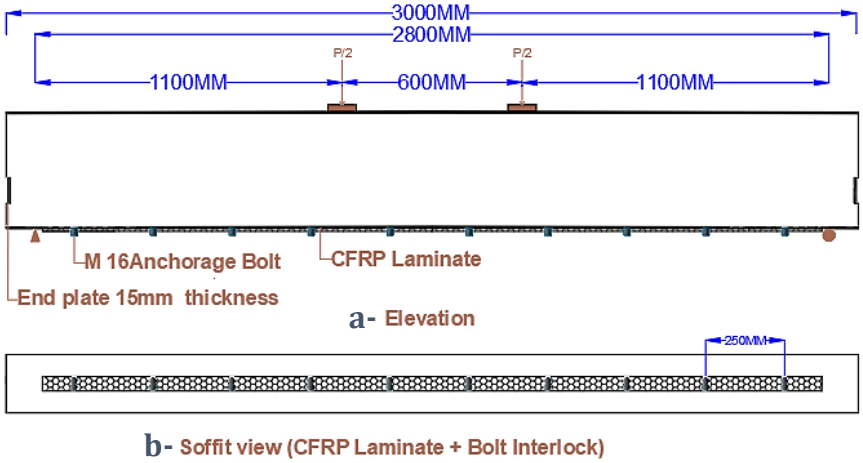

Figure 7. Laminate and mechanical bolts anchorage, a- elevation b- soffit view

The first letter, "M" in the specimens' identity in **Table 1** below, stands for a structural member, while the “R” letters stand for reference, the "S" letter for CFRP laminate strengthening, and the "W" letter for the end anchorage wrapping strengthening, "C" refer to the end with middle anchorage wrapping strengthening. Letters “I” and “B” refer to the interlock and mechanical bolt anchorage, respectively.

Table 1. Member details

Member ID	Aps (mm^2)	Laminate (L_f)			Sheets (S_f)			ρ_p (%)	ρ_s (%)
		t_{Lf} (mm)	b_{Lf} (mm)	L_{Lf} (m)	t_{sf} (mm)	b_{sf} (mm)	L_{sf} (mm)		
M0	197.40	-----	------	-----	------	------	-----	0.490	0.810
MR	169.20	-----	------	-----	------	------	-----	0.385	
MS		1.2	50	2.7	------	------	-----		
MSW		1.2	50	2.7	70.1	025	75		
MSWC		1.2	50	2.7	70.1	500	75		
MSI		1.2	50	2.7	------	------	-----		
MSB		1.2	50	2.7	------	------	-----		

2.1 Properties of Tested Member

Portland cement f'_c =45MPa with 480 kg/m^3 of cement, 725 kg/m^3 of sand, 1050 kg/m^3 of gravel, and 145l/m^3 of water in addition to 4.5 L/m^3 of superplasticizer (PC200). The properties of used steel reinforcement are 577 MPa for the yield strength, 710MPa for ultimate strength, and 13.4% for the elongation of longitudinal rebars, while 517 MPa, 659MPa, and 12.1% for the yield strength, ultimate strength, and elongation respectively for stirrups. (Steel modulus of elasticity equal to 200,000 MN/m^2). The properties of strand grade 270 used were 137 kN for minimum load at 1%, 191 kN ultimate tensile force with a modulus of elasticity equal to 197500 MPa. In addition to the resin, the manufacturer supplier provided the properties of carbon fiber fabrics (mechanical and physical), which included the nominal thickness, tensile strength, and ultimate elongation values of 0.012 m, 3100 MPa, and 0.02 for laminate (modulus of elasticity equal to 170000 MPa) for laminate. For the unidirectional sheet, the properties were 0.17mm, 3500 MPa, and 2.1% (modulus of elasticity equal to 230000 MPa).

2.2 Electronic Strain Indicator

A unidirectional electronic strain indicator was fitted to each member's middle length to monitor strain in the concrete, strand, FRP, and steel.

3. EXPERIMENTAL TESTING AND RESULT

The steel cages were equipped with electric strain gages before being inserted in a mould made for Plywood for casting reinforced concrete. Utilize ready-mixed reinforced concrete. As illustrated in **Fig. 8.** As well as for the camber measuring the dial indicator fixed at the mid-span, the electronic strain indicator’s wires were connected to the strain data acquisition device (Datalogger) to record the strand ‘s strain throughout the prestressing operation.

(a) (b) (c)

Figure 8. Operation of post-tensioning, a-PS equipment; b- PS process; c- camber recording

Table 2. Electronic strain indicator

Code	Adhesive	QTY. location	Ohm. Ω	Usage
FLAB–6–11	CN	1 @ tension bars	118.5±0.5	Steel
YEFLAB-2-3	CN	4 @ mid-span	119.5±0.5	Strand
PL-60-11	CN-E	4 @ mid-span	120±0.5	Concrete
BFLAB-5-3	CN	2 @ soffit laminate	119.5±0.5	CFRP

At the lateral ends, two- steel plates 10mm thick were utilized to guide and protect the strain indicator wires during the prestressing procedure, with a 22.5mm-diameter hole cut in each endplate for PS strand ducting. For the un-grouted strands, anchorage and split-wedge anchor grips (of the barrel variety) were utilized. The lateral grips were affixed to the strands and restricted with an end plate, then marked with a Marker pen to indicate the amount of pre-strain applied to each strand. (Change in length is 155 mm as specified by the member design) In two phases, the first left strand was pulled out to the required prestressing value: first for strand extension and then to the desired prestressing value. (L), released the jack and repeated the procedure with the second right strand. Using pressure gauge pointing from the hydraulic pressure jack utilized for post-tensioning.

Two dial indicators are fitted to each lateral end of the strand to measure strand slippage during the loading procedure. Four LVDTs were used to record the displacement of the tested members; two of them are fixed 10cm away from support, one below the mid-span, and the fourth set up at the quarter of a percent; all LVDTs were calibrated to zero strains at the start of the test, as depicted in **Figure 9**.

Figure 9. Member setup on the tested frame

To incrementally boost the load, a hydraulic jack with a capacity of 50 tons was installed at the top of a load cell, and 15 kN increments were considered as loading steps until the breaking load capacity was reached. Then the load increased by increments of 30 kN until failure occurred. The testing of each beam requires around 130 to 170 minutes. The load cell indicator was utilized to record each increment of applied load coming from the experimental frame of the test as well as to gather the massive reading data output, which gives output data for the load as it was continuously applied from the frame indicated for each load step after the fracture emerged. After the test, two sides fracture pattern of the cross-section was taken and marked with markers. Failure modes and ultimate loads were given for each instance. During the experimental testing, the first crack, the crack pattern illustrated in Fig. 10, and load-deflection were observed.

3.1 Flexural Capacity and Load-Displacement

As depicted in **Figure 11** below, tested members were examined at three different distinct load stages: cracking loads, post-cracking elastic stage, and ultimate loads capacity. When the applied load is below the cracking load value, the laminates (CFRP) and tendons do not impact the specimen's behavior. The results show that they lose strength when compared to the control member (undamaged); however, the reinforced members with laminated showed an improvement in the flexural capacity of 13%, and member strengthening with laminate and different anchorage techniques varies from 22%, up to 29%, implying the sound of the using of anchorage effect on the enhancement of strength and ductility due to the impact of delaying of debonding between longitudinal laminate and concrete surface **Table 3**.

The stiffness of the reference girders drops marginally, while the stiffness of the reinforced members is not much different from that of the damaged girders. When the applied loads from the testing frame for flexural strength increase and surpass the value of the cracking load, the member that is exposed to 14.3% of the cutting strand exhibits a relatively high value of stiffness drop due to the lack of a portion of the pre-stressing flexural force, which increases the average of crack and displacement development. Similarly, the flexural CFRP strengthening EB of the laminates demonstrate their ability to delay the fracture formation and stiffness degradation of the strengthened girders, and the girders strengthened with laminates and debonding-enhanced anchors are observed to be superior to the girders strengthened with laminates alone.

According to the control result, the displacement at the serviceability limit (L/250) is 11.2mm, and this value is pointed as the permitted load, which is approximately 78.5% of the maximum load. During this stage, the displacement of the reinforced girders was exposed to a 10% reduction for MS and about 15% for the anchorage members. It should be figured out that in each instance, the member with the anchoring has a smaller load drop, substantially greater stiffness, and greater strength. The CFRP girders strengthened with CFRP laminate and different types of anchorage exhibit an increase in deflection at the maximum load due to the lack of a relatively gradual decrease in load after the onset of partial degradation, as well as the ability of the members with an anchor to keep their ductile response. The ultimate displacement increased significantly when the specimens were strengthened with laminates alone and laminated with anchorage.

Table 3. Summary of testing result

Member code	Loading at Cracking level (kN)	Changing in Cracking load %	Maximum Load (kN)	Mid-span displacement @ maximum load (mm)	P_{cr}/P_{ult} (%)	Flexural capacity changing(%)		Failure mode
M0	55	----------	166	27	33.1			SF, CC
MR	52	5.8	157	26	33.1	5.4	Reduction	SF, CC
MS	62	14	188	24	33.4	13	Increase	SF, CC-DC
MSW	66	21	202	28	33.0	22	Increase	SF, CC-CD
MSWC	70	29	214	29	33.0	29	Increase	SF, CC-CD
MSI	67	21	199	27	33.5	20	Increase	SF, CC-CD
MSB	68	24	210	29	32.5	26	Increase	SF, CC-CD
Failure of steel at tension zone (SF), concrete crushing failure (CC), failure due to delamination of CFRP laminate (DC), failure due to covers delamination (CD).								

Figure 10. Crack pattern for the members

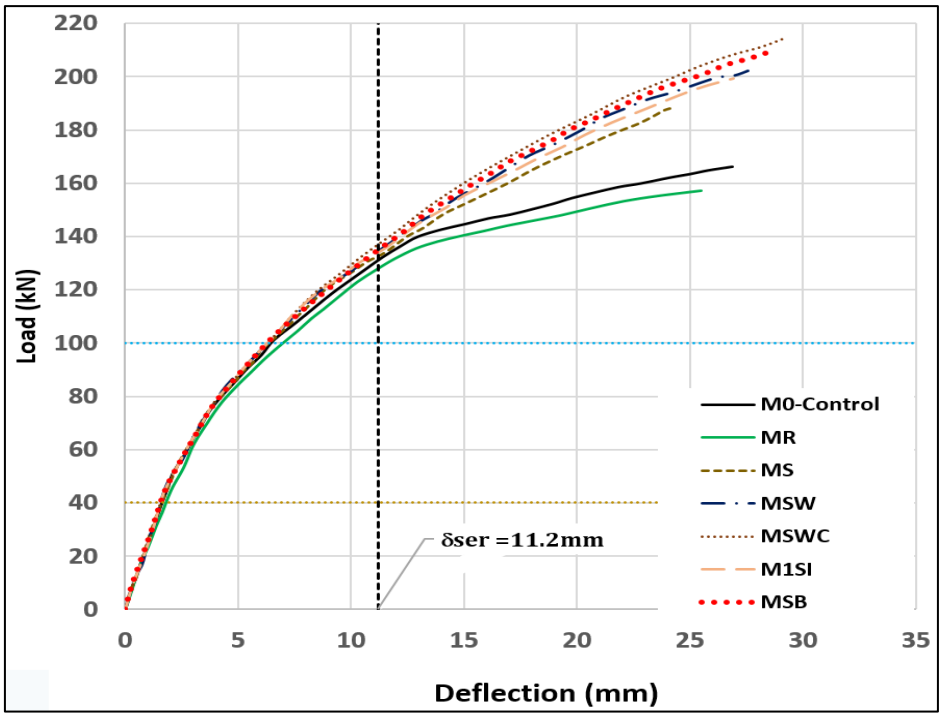

Figure 11. Load vs. displacement curve

3.2 Strain for the CFRP Laminates Verse Applied Load.

Before the cracking load, the strain in CFRP laminates in **Figure 12** below is minimum and almost equal. After the load exceeds the breaking threshold, the strain visibly increases, and after the tension rebar yields, the average strain increase expedites dramatically. The increased strain average in laminates made from carbon fibre-reinforced polymer with or without anchorage techniques was nearly identical, but the ultimate strain of the strain increases in carbon fibre-reinforced polymer laminates with anchors was significantly more than its counterpart in those members without anchorage. At the serviceability load stage, the strain increases of strengthened designed members MS was 0.27%, which corresponded to 13.3% of the strain rate of laminate capacity (ultimate breaking =2%) with no significant change to the specimen that was strengthened with laminate and anchorage MSW, MSWC, MSI, and MSB. In contrast, the strain increase at the ultimate loads was 1% for MS, corresponding to 41.5 % of the maximum strain of the fiber elongation capacity.
In contrast, the specimens strengthened with laminate anchorage demonstrated more strain at the ultimate load. In addition, using FRP laminates with anchorage had an essential effect on the compressive concrete zone strain. As previously described, the CFRP laminates can prevent the formation of cracks in their course.

3.3 Applied load verse strand strain

Due to the insignificant strain increases, the strand wasn't contributing to flexural strength before the onset of the first crack. The change in strand strain was estimated by subtracting the initial effective strain after prestressing (4,500 micro-strains) from the strain value recorded. **Figure 12**. The strand behaved identically in all investigated members over this loading phase. The increased strain in the strand for the damaged member was more than

in the undamaged girder. However, the increased strain in the strand for the members reinforced with CFRP laminate was smaller than the strain increases in the strand for the unreinforced member. At the serviceability stage, the increase in strand strain for members MR was 7500, representing an increase of about 9%, compared to the undamaged member. Similarly, the strain increments in the strands of the reinforced member's MS 6750, with a decrease of 15% compared to the parallel strain increases in the damaged member references.

Compared to the control and damaged girder, the reinforced member's MS showed substantially less strand strain increases in the loading level following the load in the level of serviceability than the control and damaged members. Increases in tendon strain were reduced by 14.67% for B1SW when end anchors were utilized. All of the results mentioned above and analyses have demonstrated that the carbon fibre-reinforced polymer strengthened by laminates, including anchors, has a presumed effect on the attitude of the strands. As indicated before, the CFRP laminates could postpone and avoid the evolution of cracks, as well as slow the loss of member stiffness.

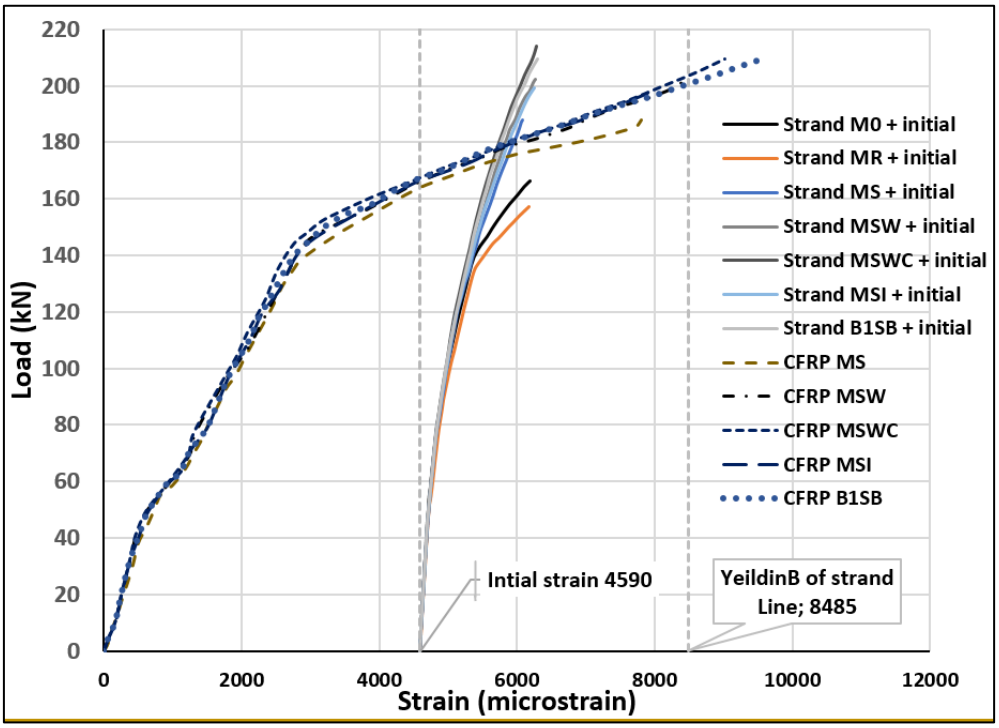

Figure 12. Load Vs. the strain of CFRP and PS

4. MOMENT CAPACITY PREDICATION

Determining the increase in a strain of unbonded strands is crucial for determining the strength development of un-grouted post-tension members reinforced with externally attached carbon fiber-reinforced polymer laminates. Unfortunately, the design guidelines, such as (ACI Committee 440-2R 2017), have only suggested a method for evaluating the increase in a strain of bonded post-tensioned and pre-tension members strengthened with EB-CFRP laminates, while the corresponding methods for un-grouted stands in members reinforced with CFRP laminates have not been included (**Al-Zuhairi and Sahi, 2013**). In addition, experimental findings demonstrated that carbon fibre-reinforced polymer

composites considerably affect the attitude of unbonded tendons **(Naqi and Al-zuhairi, 2020)**. The change in the strain of the strand of the unbonded post-tension member reinforced with CFRP was determined using **(Nguyen-Minh et al., 2018)** formulae for unbonded tendons in typical reinforced concrete components, as below.

$$M_n = A_{ps} f_{ps} \left(d_p - \frac{\beta_1 c}{2}\right) + A_s f_s \left(d - \frac{\beta_1 c}{2}\right) + \Psi_f A_f E_f \varepsilon_f \left(d_f - \frac{\beta_1 c}{2}\right) \quad (1)$$

$$\varepsilon ps = \varepsilon_{pe} + \varphi_{ps}\, N_p\, \varepsilon_c \left(\frac{d_p - c}{L_a}\right). \quad (2)$$

where:

Initial strand's strain, $\varepsilon_{pe} = fse \,/\, Eps$ excluding stress losses,
The strain of the prestressed strand, ε_{pe} (microstrain).
The strain of the carbon fiber, ε_f (microstrain).
Modulus of elasticity of the carbon fiber, E_f (MPa).
Modulus of elasticity of the prestressing strand, E_{ps} (MPa)
The distance from carbon fiber to the top of the cross-section, d_f (mm)
The distance from the strand to the top of the cross-section, d_p (mm)
The distance from rebars to the top of the cross-section, d (mm).
Tensile and compressive rebar stress, *fs*, (MPa)
Effective stress of strand, f_{se} (N/mm^2), which is equal to the force over an area (F_p/A_p)
Tendon's actual tension force, F_p (N)
Strand cross-sectional area, A_{ps} (mm^2)
Rebars cross-sectional area, A_s (mm^2)
The cross-sectional area of carbon fiber, A_f (mm^2), equals t_{Lf} times b_{Lf}.
φ_{ps}: stands for the stress reduction factor and has a value of 10.5 when applied by (Tam and Pannell 1976), while **(El Meski and Harajli, 2013)** suggest the value to be 0.70, and this value has been considered.
φ_f: stands for the carbon fiber reduction factor, which was determined to be 0.85 according to (ACI Committee 318-19 2019)
Np: is the parameter that is set to 14.0 as the constant value, is taken into consideration for simple end beams **(El Meski and Harajli, 2013)**, which is a unit less factor
A span of the tested girder, La (mm)
Table 4 and **Figure 13** exhibit the predicted-to-experimental flexural strength ratios Mu, predicated /Mu, and experimental. The "mean value" Avg. = 94% and "coefficient of variance" COV = 5.1% describe the precision of predicated flexural strength values and their applicability for predicting the flexural CFRP strength EB reinforced unbonded prestressed concrete member including or does not include and without anchorages.

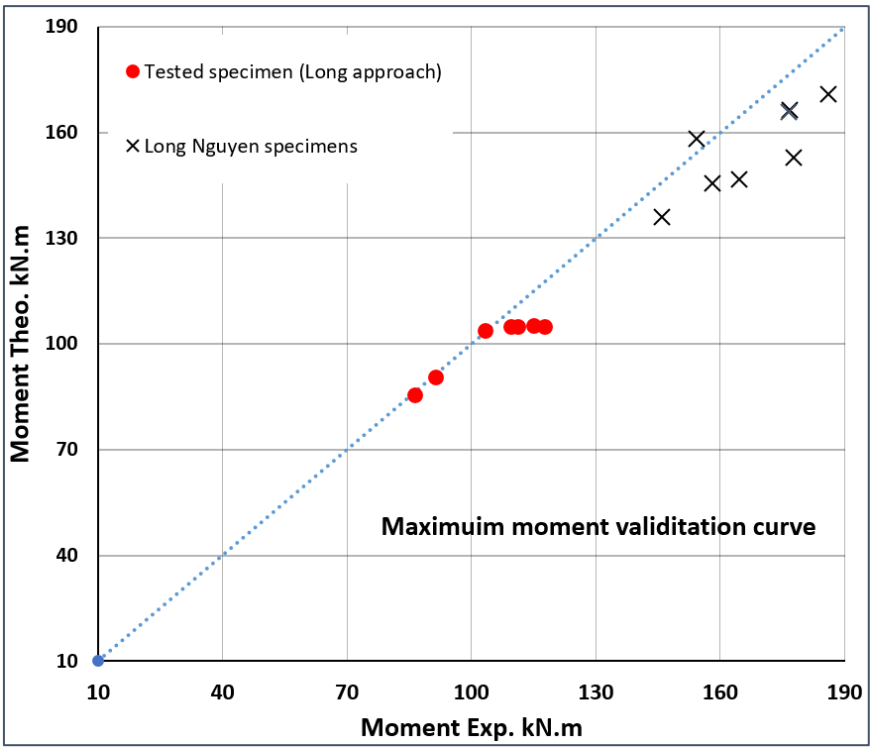

Figure 13. Flexural capacity experimental and predictions result

Table 4. Predicated VS experimental result

No.	(Nguyen-Minh et al., 2018) members				Tested members			
	Member-code	Exp. Moment	Pred. Moment	$\frac{M_{pred.}}{M_{exp.}}$	Member-code	Exp. Moment	Pred. Moment	$\frac{M_{pred.}}{M_{exp.}}$
1	M2CB	145.90	136.00	0.93	MO-Control	91.43	90.552	0.99
2	M4CB	154.30	158.20	1.03	MR	86.49	85.327	0.99
3	M6CB	177.70	152.80	0.86	MS	103.39	103.763	1.00
4	M2CB-	164.60	146.60	0.89	MSW	111.17	104.929	0.94
5	M4CB-	176.70	165.50	0.94	MSWC	117.76	104.885	0.89
6	M6CB-	186.10	170.80	0.92	B1SFW	120.94	104.885	0.87
7	M2CB-	158.00	145.60	0.92	MSI	109.64	104.923	0.96
8	M4CB-	176.70	166.40	0.94	MSB	115.20	104.962	0.91
Mean (M)				0.93				0.94
SD- standard Deviation				0.049				0.048
COV- coefficient of variation				51%				53%
Testing girder vs. **(Nguyen-Minh et al., 2018)**								
Mean (M)								0.94
Standard Deviation (SD)								0.05
Coefficient of variation (COV)								51%

5. CONCLUSIONS

The results obtained in this paper are based on the experimental findings and the proposed analytical method. These models were developed to predict the amount of ultimate load restoration for the damaged members using the anchorage techniques that enhanced the bonding strength and increased the load-carrying capacity.

• Members equipped with the proposed anchorage exhibited an approximately 15% greater debonding load and a higher maximum load and associated deflection. Anchors received more CFRP strain than their equivalent members without anchors, and the maximum strain is significantly greater than that predicted by theory. It was revealed that the anchorage is effective at restricting the degree of debonding of the longitudinal CFRP laminate, hence contributing (indirectly) to the flexural stiffness of the member by limiting the crack width.

• For a given loading value, the flexural capacity of damaged post-tensioned girders is less than the undamaged member, and the displacement of the damaged strand is greater than the undamaged strand. The test results showed revealed flexural capacity losses up to for damaged strands 5.4% at midspan, and for a reinforced member, the flexural capacity is regained and increased by the amount of strength lost due to the damaged strand (13%, 22%, 29%, 20%, and 26% for BS, BSW, BSWC, BSI, and BSB respectively).

• The best anchorage proposed techniques were found in the use of CFRP sheet at the end and the center due to the participation of the sheet in delaying the debonding, restricting the cracks, increase stiffness more than other techniques.

• The suggested equations for tendon strain increase calculation in unbonded prestressed reinforced concrete elements reinforced with EB-CFRP laminates predict flexural capacity with low variance and high precession (Mean equal to 0.94 and COV similar to 0.051).

REFERENCES

Abbas, H.Q., and Al-Zuhairi, A.H., 2022. Usage of EB-CFRP for improved flexural capacity of unbonded post-tensioned concrete members exposed to partially damaged strands. *Civil Engineering Journal*, 8(6), pp. 1288-1303. Doi:10.28991/CEJ-2022-08-06-014.

Abbas, H.Q., and Al-Zuhairi, A.H., 2022. Flexural strengthening of prestressed girders with partially damaged strands using enhancement of carbon fiber laminates by end sheet anchorages. *Engineering, Technology & Applied Science Research*, 12(4), pp. 8884-8890. Doi:10.48084/etasr.5007.

Abdulkareem, B.F., and Izzat, A.F., 2022. Serviceability of post-fire RC rafters with openings of different sizes and shapes. *Journal of Engineering*, 28(1), pp. 19-32. Doi:10.31026/j.eng.2022.01.02.

Abdulkareem, B.F., Izzet, A.F., and Oukaili, N., 2021. Post-fire behavior of non-prismatic beams with multiple rectangular openings monotonically loaded. *Engineering, Technology & Applied Science Research*, 11, pp. 7763-69. Doi:10.48084/etasr.4488.

ACI Committee 318-19. 2019. Building Code Requirement for Reinforced Concrete. *American Concrete Institute*.

ACI Committee 440-2R. 2017. Guide for the Design and Construction of Externally Bonded FRP Systems for Strengthening Concrete Structures. *American Concrete Institute*.

Al-Hilali, A.M., Izzet, A.M., and Oukaili, N., 2022. Static Shear Strength of a Non-Prismatic Beam with Transverse Openings. *Engineering, Technology & Applied Science Research*, 12, pp. 8349-8353 Doi:.10.48084/etasr.4789.

Al-Zuhairi, A.H., Sahi, W.D., 2013. Numerical Prediction of Bond-Slip Behavior in Simple Pull-Out Concrete Specimens. *Journal of Engineering*, 19(1), pp. 1-12. Doi:10.31026/j.eng.2013.01.01

Daraj, A.J., and Al-Zuhairi, A.H., 2022. The Combined Strengthening Effect of CFRP Wrapping and NSM CFRP Laminates on the Flexural Behavior of Post-Tensioning Concrete Girders Subjected to Partially Strand Damage. *Engineering, Technology & Applied Science Research*, 12, pp. 8856-63. Doi:10.48084/etasr.5008.

El Meski, F.M., and Harajli, M.H., 2013. Flexural Capacity of FRP Strengthened Unbonded Prestressed Concrete Members: Proposed Design Guidelines. 11th International Symposium On Fiber Reinforced Polymers For Reinforced Concrete Structures (FRPRCS-11), 26-28 June 2013, hosted by University of Minho and ISISE, Guimarães, Portugal.

Hekmet, HM, and AF Izzet. 2019. Performance of segmental post-τensioned concrete beams exposed to high fire temperature. *Engineering, Technology & Applied Science Research*, 9(4), pp. 4440-4447. Doi:10.48084/etasr.2864.

Jalil, A., and Al-Zuhairi A.H., 2022. Behavior of Post-Tensioned Concrete Girders Subject to Partially Strand Damage and Strengthened by NSM-CFRP Composites. *Civil Engineering Journal*, 8(7), pp. 1507-21. Doi:10.28991/CEJ-2022-08-07-013.

Naqi, A.W., and Al-zuhairi, AH.. 2020. Nonlinear finite element analysis of RCMD beams with large circular opening strengthened with CFRP material. *Journal of Engineering*, 26(11), pp. 170-183. Doi:10.31026/j.eng.2020.11.11.

Nguyen-Minh, L., Phan-Vu, P., Tran-Thanh, D., Thi Truong, Q.P., Pham T.M.,, Ngo-Huu, C., and Rovňák. M., 2018. Flexural-strengthening efficiency of cfrp sheets for unbonded post-tensioned concrete T-beams. *Engineering Structures*, 166(1), pp. 1-15. Doi:10.1016/j.engstruct.2018.03.065.

Oukaili, N., and Buniya, M.K., 2013. Serviceability performance of externally prestressed steel-concrete composite girders. *Journal of Engineering*, 19(6), pp. 734-751. Doi:10.31026/j.eng.2013.06.06.

Razaqpur, G., and Mostafa, A.B., 2015. C-Anchor for strengthening the connection between adhesively bonded laminates and concrete substrates. *Technologies*, 3(4), pp. 238-258. Doi:10.3390/technologies3040238

Tam, A., Pannell, F.N., 1976. The ultimate moment of resistance of unbonded partially prestressed reinforced concrete beams. *Magazine of Concrete Research*, 28(97), pp. 203-08 Doi:10.1680/macr.1976.28.97.203.